Journal of Polymers and the Environment (2022) 30:4863–4876
https://doi.org/10.1007/s10924-022-02529-8

ORIGINAL PAPER

Ion Imprinted Sodium Alginate Hydrogel Beads Enhanced with Carboxymethyl Cellulose and β-Cyclodextrin to Improve Adsorption for Cu^{2+}

Yajun Fan[1] · Dianling Shen[1] · Yu Yan[2] · Xiaopeng Hu[1] · Yaping Guo[1] · Yujun Zhong[1] · Zhiyang Li[1] · Lianwu Xie[1,2]

Accepted: 1 July 2022 / Published online: 1 September 2022

Abstract

To achieve efficient adsorption and recycling of Cu^{2+} in wastewater, using Cu^{2+} as template ion, glutaraldehyde as crosslinker, three sodium alginate hydrogel beads including SA, SAC, and SAB beads were prepared by imprinting sol–gel method using sodium alginate (SA) with carboxymethyl cellulose (CMC) and β-cyclodextrin (β-CD) as different precursors, respectively. Scanning electron microscopy and Fourier transform infrared spectroscopy were used to characterize and analyze morphology and composition change of the hydrogel beads, respectively. When the mass ratio of SA to CMC or SA to β-CD reach 1:1, the SAC beads or SAB beads are nearly homogeneous sphere. Then the effects of pH, adsorption time, initial concentration of Cu^{2+}, adsorbent dosage, and coexisting ions on the adsorption efficiency of three hydrogel beads were investigated. The results indicated that adding carboxymethyl cellulose and β-cyclodextrin into skeleton of beads increased the toughness of the beads and improved the adsorption capacity of Cu^{2+}. Compared to the saturated adsorption capacity 510 mg/g of Cu^{2+} on SA, the saturated adsorption capacity of Cu^{2+} on SAB and SAC reached 817 mg/g and 822 mg/g, respectively. And their adsorption efficiency for Cu^{2+} are over 95% at 25 °C with pH of 7, contact time within 350 min, adsorbent dosage of 4 mg/50 mL, and initial concentration of 5 mg/L. Thus, SAC and SAB beads could be used as adsorption material for detecting and removing Cu^{2+} from wastewater.

Keywords Sodium alginate · Carboxymethyl cellulose · β-Cyclodextrin · Copper ions · Ion imprinted hydrogel beads · Specific adsorption

Introduction

With the development of modern industry, wastewater polluted by heavy metals from the manufacture of pesticides, fertilizers and metals has become an important field of environmental treatment [1–3]. The non-degradability of heavy metals in soil and water makes them accumulate in organisms, which leads to organism damage and finally endangers human life and health [4]. Therefore, the efficient treatment of heavy metals has always been the key point of national environmental protection [5]. China has established a series of discharge standards for heavy metals in aquatic ecosystem. For example, the comprehensive sewage discharge standard GB 8978–1996 stipulates that the maximum acceptable emission concentration of Cu^{2+} is 0.5 mg/L. Copper is an essential trace element for human body. However, excess accumulation of Cu^{2+} in human body through food chain will cause damage to liver, heart, lung, and brain, and threaten the safety of human life. Various ecological problems caused by copper pollution have also received great attention from relevant environmental protection departments. Therefore, effective removal of copper from polluted water bodies has always been an important topic for scientific researchers and governors.

The treatment methods for heavy metals including Cu^{2+} in wastewater include: chemical method [6], adsorption [7, 8], electro-dialysis [9, 10], ion exchange method [7, 11],

✉ Yaping Guo
guoyaping@csuft.edu.cn

✉ Lianwu Xie
xielianwu@csuft.edu.cn

[1] College of Sciences, Central South University of Forestry and Technology, Changsha 410004, China

[2] College of Material Science and Technology, Central South University of Forestry and Technology, Changsha 410004, China

photocatalysis methods [12, 13]. Various chemical method such as chemical precipitation are being used for the treatment of wastewater containing Cu^{2+}, but still are limited in their efficiencies, residues, cost, and versatility [14]. Electrodialysis method has been recognized as an efficient treatment for the wastewater, but it is unsuitable for distressed area lack of electric power [15]. The ion-exchanger with good ion exchange capacity, chemical stability, and thermal stability [16], would inevitably bring another ion into wastewater after treatment. Photocatalysis has been an interesting issue for the degradation of organic contaminants and heavy metals for quite a few years. However, many photocatalysis materials hold the disadvantage of photo-corrosion which decline the photoactivity and stability [17]. With the adsorption method's advantages such as economical, simple and easy to handle, and wide scope of application [18], the research and development of green adsorption materials with good performance and specific selectivity is becoming an important trend of controlling pollution and recycling of heavy metals [19–22].

The ion-imprinted polymer is regarded as one type of green adsorption materials with specific selectivity [23]. Ion imprinting technology is the technique that creating three-dimensional cavity structures in a polymer matrix, i.e., ion imprinting polymers by the copolymerization of functional monomers and cross-linkers in the presence of target ion as template ion based on coordination or electrostatic interactions. After removal of the template ion with acidic reagent, recognition cavities complementary to the template ion were formed in the highly cross-linked polymer matrix [24]. Except for inorganic reagent such as 3-aminopropyltriethoxysilane, some natural raw materials such as chitosan and sodium alginate were used as the functional monomer to prepare ion-imprinted polymer. When using sodium alginate as functional monomer, ion-imprinted hydrogel beads could be easily obtained owing to its good film forming property [25]. The hydrogel beads have the advantages of degradable, good biocompatibility, high load, high specific surface area, convenient operation and transportation, etc. However, ion-imprinted sodium alginate hydrogel beads are rarely studied.

Sodium alginate (SA) is a natural macromolecular polysaccharide extracted from brown algae and composed of α-L-glucuronic acid and β-D-mannouronic acid. It is water-soluble and contains a large number of free carboxyl groups that can interact with heavy metal ions. Thus, it can be used as an excellent adsorption material for heavy metals [26, 27]. And β-cyclodextrin (β-CD) with a circular structure formed by the α-1,4-glycosidic bond connecting seven D-glucopyranose basic units, contains a cavity structure that can encapsulate ions and organics, etc., and its molecular surface contains a large number of hydroxyl groups that can chelate with heavy metal ions to form complexes [28–30]. Carboxymethyl cellulose (CMC) is a renewable natural cellulose ether compound, which contains abundant hydroxyl and carboxyl groups and can form hydrogels through physical or chemical methods [23, 31].

In this paper, to achieve efficient adsorption of Cu^{2+} from wastewater, using Cu^{2+} as template ion, glutaraldehyde as crosslinker, three kinds of sodium alginate hydrogel beads were prepared by imprinting sol–gel method using SA with CMC and β-CD as different precursors, respectively. Two of them were enhanced with CMC and β-CD to improve adsorption for Cu^{2+}. Scanning electron microscopy (SEM) and Fourier transform infrared spectroscopy (FT-IR) were used to characterize and analyze the sodium alginate hydrogel beads, and the influence of different factors on adsorption performance of the hydrogel beads was also investigated. Some adsorption experiments and different adsorption kinetics models were used to analyze the adsorption mechanism of Cu^{2+} on the hydrogel beads.

Materials and Methods

Chemicals and Apparatus

Sodium alginate (Chemically Pure, C.P.), carboxymethyl cellulose (C.P.), β-cyclodextrin (C.P.), glutaraldehyde (25%, Biochemical Reagent, B.R.), hydrochloric acid (38%, A.R.), and sodium hydroxide (A.R.) were all purchased from Sinopharm Chemical Reagents Co., Ltd. Anhydrous copper chloride (99.99%) was purchased from Shanghai Aladdin Biochemical Technology Co., Ltd. Triple distilled water was used in the experiment.

The instruments and equipment used in this paper mainly included QUANTA FEG 250 field emission environmental scanning electron microscope (FEI Co., OR, USA), Nicolet iS5 Fourier transform infrared spectrometer (Thermo Fisher Scientific, MA, USA), Optima 8000 inductive coupled plasma (ICP) emission spectrometer (Perkin-Elmer, MA, USA), SZ-97 automatic triple water distiller (Yarong Biochemical Instrument Co., Shanghai, China), PXSJ-226 pH meter (INESA Instrument Co., Shanghai, China), AL204 electronic analytical balance (Mettler Toledo Instrument Co., Zurich, Switzerland), TL-F6 micro injection pump (Tongli Weina Co., Shenzhen, China), and HYG-A shaker (Taicang Equipment Co., Jiangsu, China).

Preparation of Sodium Alginate Hydrogel Beads

The structural stability and the adsorption effect of sodium alginate hydrogel beads on Cu^{2+} were improved by adding different precursors. The effects of concentrations of precursors and concentration of template Cu^{2+} on the pellet formation of hydrogel beads were investigated in the preliminary stage, and Cu^{2+} pre-adsorption experiments

were conducted to obtain the optimal conditions for the preparation of sodium alginate hydrogel beads by imprinting sol–gel method.

Preparation of SA Hydrogel Beads

The SA hydrogel beads were synthesized by the following procedure. SA (2.0 g) was added into 200 mL distilled water with a magnetic stirrer for 6 h at 25 °C. Then, 4 mL glutaraldehyde solution (as crosslinker) in H_2O (25%, *w*/*w*) was added into above solution and reacted at 25 °C for 12 h under sealing and stirring to prepare sol solution. The prepared sol solution was dropped into 200 mL 0.2 mol/L Cu^{2+} aqueous solution by a micro-injection pump at a constant rate to obtain hydrogel beads, and the hydrogel beads were stabilized by Cu^{2+} ion imprinting for 10 h. After washing the hydrogel beads with distilled water for 5 times (50 mL each time), SA hydrogel beads (abbr. as SA beads) were obtained by eluting Cu^{2+} in the hydrogel beads with 100 mL 0.5 mol/L HCl for 5 times and washing with 50 mL distilled water for 5 times. The proposed reaction was shown in Scheme 1a.

Preparation of SAC Hydrogel Beads

The mass ratio of SA to CMC is an important factor in the preparation of SA + CMC hydrogel beads (abbr. as SAC beads). At preliminary experiment, we investigate the effect of mass ratio of SA to CMC (from 4:1 to 1:4) on morphology of hydrogel beads. The hydrogel beads are nearly homogeneous sphere once the mass ratio of SA to CMC reach 1:1. Then, the SAC hydrogel beads were synthesized by the following procedure. SA (3.0 g) and CMC (3.0 g) were added into 200 mL distilled water with a magnetic stirrer for 6 h at 25 °C. After the same subsequent treatment as the "Preparation of SA Hydrogel Beads" section, the SAC beads were obtained. The proposed reaction was shown in Scheme 1b.

Preparation of SAB Hydrogel Beads

As "Preparation of SAC Hydrogel Beads" section, when the mass ratio of SA to β-CD reach 1:1, the SA + β-CD hydrogel beads (abbr. as SAB beads) are nearly homogeneous sphere. Then, the SAB hydrogel beads were synthesized by the following procedure. SA (3.0 g) and β-CD (3.0 g) were added into 200 mL distilled water with a magnetic stirrer for 6 h at 25 °C. After the same subsequent treatment as the "Preparation of SA Hydrogel Beads" section, the SAB beads were obtained. The proposed reaction was shown in Scheme 1c.

Structure Characterization for Hydrogel Beads

All sodium alginate hydrogel beads were freeze-dried (– 80 °C) before structure characterization in order to avoid damaging the structure by drying in normal oven. SEM was used to characterize the morphology of the hydrogel beads, and FT-IR was used to characterize the composition change of the hydrogel beads.

Adsorption Experiment

Adsorption experiment was conducted to investigate the effects of different experimental parameters on the adsorption of Cu^{2+} on the hydrogel beads. A fixed amount of the sodium alginate hydrogel beads was added into a series of Cu^{2+} solution with different concentration, respectively. Then the solution was oscillated for adsorbing 12 h at 120 r/min in a shaker under different temperature. After that, the concentration of Cu^{2+} in the solution reaching equilibrium adsorption was determined by the inductive coupled plasma emission spectrometer (ICP). All the adsorption experiments were repeated for three times and the mean values were recorded. The adsorption capacity and adsorption efficiency of the sodium alginate hydrogel beads were calculated according to Eqs. (1) and (2), respectively.

$$q = \frac{(C_0 - C_1) \times V}{m} \tag{1}$$

where q is the adsorption capacity (mg/g) of Cu^{2+} on hydrogel beads, C_0 is the initial concentration of Cu^{2+} (mg/L) in the solution, C_1 is the concentration of Cu^{2+} (mg/L) after adsorption, V is the volume of Cu^{2+} solution (L), and m is the weight of the dry hydrogel beads (g).

$$Q = \frac{C_0 - C_1}{C_0} \times 100\% \tag{2}$$

where Q is the adsorption efficiency (%), C_0 is the initial concentration of Cu^{2+} (mg/L) in the solution, C_1 is the concentration of Cu^{2+} (mg/L) after adsorption.

Effect of pH on Adsorption

The dry hydrogel beads (4 mg) were added into 50 mL Cu^{2+} solution (5 mg/L) with different pH ranging 1–8. In a shaker, the adsorption was carried out under 25 °C at 120 r/min for 10 h to study the effect of pH on the adsorption.

Effect of Hydrogel Beads Dosage on Adsorption

The dry hydrogel beads with different weight (0.4–10 mg) were added into 50 mL Cu^{2+} solution (5 mg/L) with pH

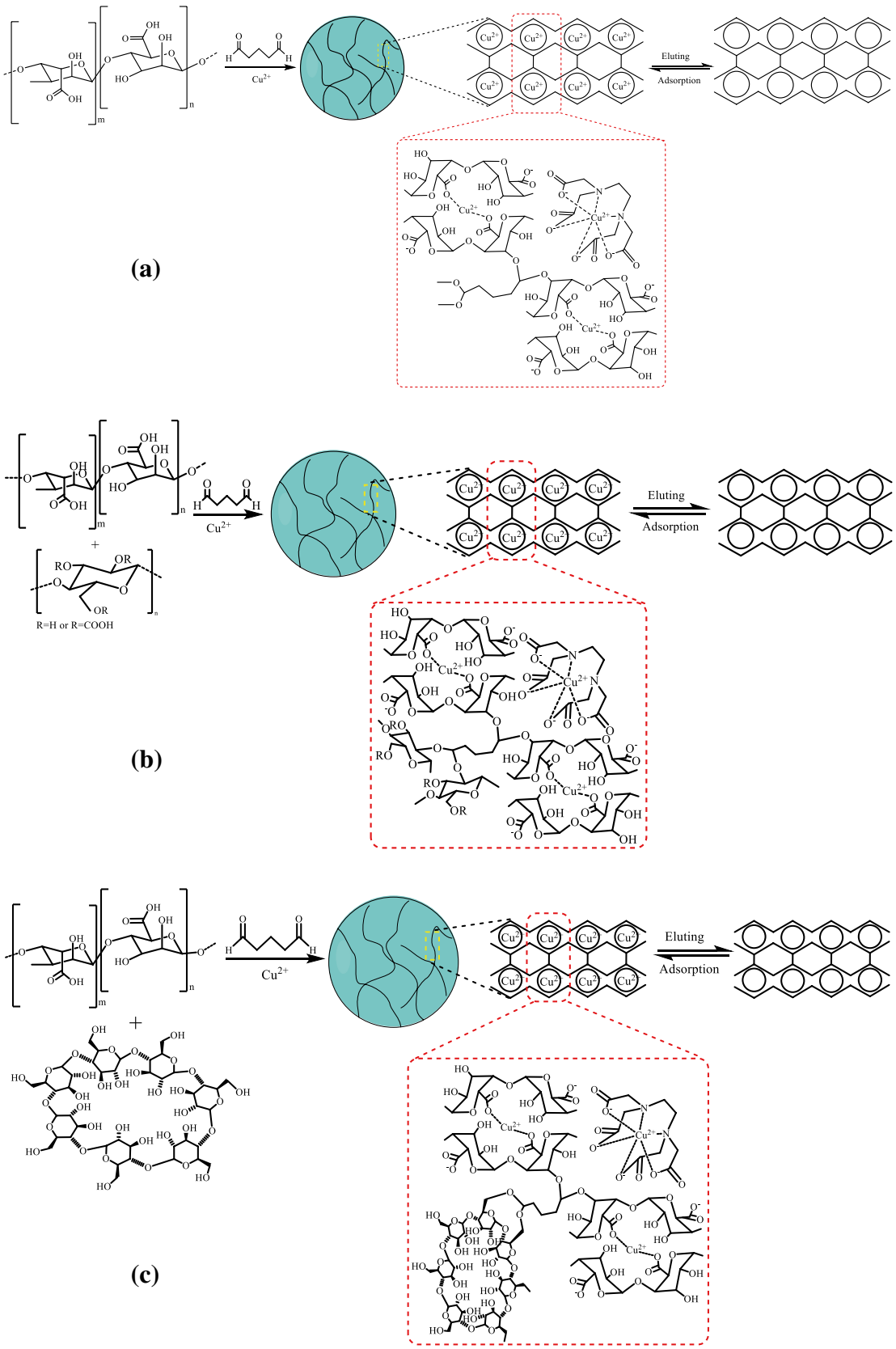

Scheme 1 The proposed preparation reaction of SA (**a**), SAC (**b**), SAB (**c**) sodium alginate hydrogel beads

7, respectively. In a shaker, the adsorption was carried out under 25 °C at 120 r/min for 10 h to study the effect of hydrogel beads dosage on the adsorption.

Effect of Initial Concentration on Adsorption

A series of Cu^{2+} solution with different concentration ranging 1 mg/L to 700 mg/L was prepared firstly. The dry hydrogel beads (4 mg) were added into above all Cu^{2+} solutions (50 mL for each one) after adjusting pH to 7, respectively. In a shaker, the adsorption was carried out under 25 °C at 120 r/min for 10 h to investigate the effect of initial concentration of Cu^{2+} on the adsorption.

Adsorption Kinetics Experiment

The dry hydrogel beads (40 mg) were added into a 50 mL Cu^{2+} solution (5 mg/L) with pH 7. In a shaker, the adsorption was carried out under 25 °C at 120 r/min. The concentration of Cu^{2+} in the adsorbing solution was measured at a certain time interval, and the adsorption effect of hydrogel beads along with different treatment time was investigated. The pseudo-first-order kinetic model and the pseudo-second-order kinetic model were used to fit the dynamic adsorption data to explore the adsorption mechanism.

The pseudo-first-order kinetic equation and the pseudo-second-order kinetic equation are shown as Eqs. (3) and (4), respectively.

$$ln(q_e - q_t) = lnq_e - k_1 t \tag{3}$$

$$\frac{t}{q_t} = \frac{1}{k_2 q_e^2} + \frac{1}{q_e} \tag{4}$$

where q_t is the adsorption capacity (mg/g) at time t, q_e is the saturated adsorption capacity at equilibrium (mg/g), t is the adsorption time (h), k_1 is the pseudo-first-order adsorption rate constant (1/h), k_2 is the pseudo-second-order adsorption rate constant [g/(mg/h)].

Adsorption Thermodynamic Experiment

For better understanding the interaction mechanism between hydrogel beads and Cu^{2+} after evaluating their adsorption capacity, both Langmuir model and Freundlich model were used to fit the experimental results. In general, the Langmuir adsorption isotherm equation is used to describe the adsorption process of monolayer adsorption. The Freundlich adsorption isotherm equation is commonly used to describe the multilayer adsorption process.

The Langmuir adsorption isotherm equation and the Freundlich adsorption isotherm equation are shown as Eqs. (5) and (6), respectively.

$$\frac{1}{q_e} = \frac{1}{K_L q_m C_e} + \frac{1}{q_m} \tag{5}$$

$$lnq_e = mlnC_e + lnK_f \tag{6}$$

where q_e is the equilibrium adsorption amount of Cu^{2+} on hydrogel beads at adsorption equilibrium (mg/g), q_m is the saturation adsorption amount of Cu^{2+} on hydrogel beads (mg/g), C_e is the adsorption equilibrium concentration of Cu^{2+} (mg/L), K_L is the parameter of Langmuir isotherm equation, which is related to the strength of adsorption capacity, and its magnitude mainly depends on the nature of adsorbent, adsorbent mass and temperature; K_f is the adsorption equilibrium constant of Freundlich isotherm equation, which indicates the adsorption amount at C per unit concentration; m is the Freundlich characteristic adsorption parameter.

Effect of Coexisting Ions on Adsorption

A mixed solution of Cu^{2+} and 15 coexisting ions (Al^{3+}, Ag^{+}, Ba^{2+}, Ca^{2+}, Cd^{2+}, Co^{2+}, Cr^{3+}, Fe^{2+}, Fe^{3+}, Li^{+}, Mg^{2+}, Mn^{2+}, Ni^{2+}, Pb^{2+} and Zn^{2+}) was prepared with the same concentration of 5 mg/L, and 50 mL mixed solution was taken to adjust pH to 7 before 4 mg dried hydrogel beads were added. In a shaker, the adsorption was carried out under 25 °C at 120 r/min for 10 h. After that, the concentration of Cu^{2+} and other coexisting ions in the adsorbing solution was measured by the ICP and the effect of coexisting ions on the adsorption of Cu^{2+} was analyzed.

The separation factors (β) were calculated according to Eq. (7).

$$\beta = \frac{Q(Cu2+)}{Q(\text{other ion})} \tag{7}$$

where $Q(Cu^{2+})$ is the adsorption efficiency of Cu^{2+} on hydrogel beads, and Q(other ions) is the adsorption efficiency of other coexisting ion on hydrogel beads.

Regeneration and Recycling

The dried sodium alginate hydrogel beads (4 mg) with adsorbed Cu^{2+} were added into 50 mL HCl solution (0.5 mol/L) for desorption for 5 h, then the beads were washed with 50 mL distilled water for 5 times. The desorbed hydrogel beads were placed into 50 mL Cu^{2+} aqueous solution (5 mg/L) again for another adsorption for 10 h, and the adsorption–desorption-adsorption process was repeated to investigate the reutilization of the hydrogel beads.

Results and Discussion

Structure Characteristics of Sodium Alginate Hydrogel Beads

SEM Morphological Characteristics

In fact, there is nearly no difference of the morphology between hydrogel beads in the presence of Cu^{2+} as ion template and hydrogel beads on the absent of Cu^{2+} (data not shown). Thus, we focused on difference of the morphology between SA hydrogel beads and SAC or SAB hydrogel beads. The SEM images of SA, SAC, and SAB sodium alginate hydrogel beads were shown in Fig. 1. Although the newly prepared sodium alginate hydrogel beads were basically spherical with diameter of 3–5 mm (Fig. 1g), the freeze-dried sodium alginate hydrogel beads were ellipsoid with particle size of 1.2–2.0 mm, and with layered and fish scale-like folds on the surface (Fig. 1a, c, e) as the reported by Ding et al. [32], indicating the existence of internal cavity. Figure 1b, d, and f showed that more fold structures appeared after adding CMC and β-CD than that of SA beads, leading to a significant increase in the specific surface area of the hydrogel beads, thus enhancing the adsorption capacity of Cu^{2+} by the SAC and SAB beads.

FT-IR Spectral Characteristics

The FT-IR spectra of SA, SAC and SAB hydrogel beads before and after adsorption were shown in Fig. 2. The absorption peaks at 3427 cm^{-1}, 3440 cm^{-1} and 3466 cm^{-1} were O–H stretching vibration peaks [33, 34]. At 3440 cm^{-1}, O–H of both sodium alginate and sodium carboxymethyl cellulose produced stretching vibration peak. The broad peak of 3466 cm^{-1} was the stretching vibration peak generated by hydrogen bond between sodium alginate and hydroxyl group on cyclodextrin. The peaks of 1740 cm^{-1} and 1370 cm^{-1} were the characteristic absorption peaks of the symmetric and asymmetric stretching vibration of COO– of sodium alginate and the C=O superimposed on sodium carboxymethyl cellulose, respectively [35, 36]. The absorption peaks at 1370 cm^{-1} and 1366 cm^{-1} were related to the C–O stretching vibration and O–H bending vibration of sodium alginate and sodium carboxymethyl cellulose [37, 38]. The absorption peak of the C=O double bond at 1738 or 1740 cm^{-1} indicated that the crosslinking agent glutaraldehyde was successfully polymerized with sodium alginate. And the peak of 2904 cm^{-1} was the C–H stretching vibration of methylene of sodium alginate [39], and the absorption peak of C–H stretching vibration at 2904 cm^{-1} was weakened by the chelation of carboxylic acid group with Cu^{2+}.

The absorption peaks' wavenumber of sodium alginate hydrogel beads did not change significantly before and after adsorption, but the intensity of absorption peaks increased or decreased slightly, which indicated that the main structure of sodium alginate hydrogel beads did not change before and after adsorption of Cu^{2+}, and perhaps treating Cu^{2+} by hydrogel beads existed not only physical adsorption but also chemical adsorption which is dominated by coordination reaction.

Evaluation on Adsorption Properties

Effect of pH on Adsorption

Batch adsorption experiments were conducted to examine the effects of solution pH, initial concentration, adsorbent dosage, and contact time (adsorption kinetics) on Cu^{2+} adsorption using SA, SAC, and SAB, respectively. The effect of pH in initial solution on the adsorption efficiency of Cu^{2+} on the three sodium alginate hydrogels was shown in Fig. 3. The adsorption efficiency of SA and SAB beads was lower than 20% at pH 1–3 while that of SAC beads reached about 40%, then the adsorption efficiency of SA and SAB beads increased sharply within pH 3–4 until more than 80% within pH 4–7, and reached the maximum values at pH 7. However, the adsorption efficiency of SA hydrogel beads reached the maximum value at pH 8. These might be caused by the positive charge on the adsorbent surface, which decreased with increasing of pH in solution [40]. Considering that Cu^{2+} will generate $Cu(OH)_2$ precipitation under alkaline conditions, the optimal pH for the adsorption of the three hydrogel beads is confined to 7.

Effect of the Dosage of Hydrogel Beads on Adsorption

In addition to initial pH, adsorbent dosage is one of the most significant parameters affecting the adsorption [41]. The influence of the dosage of SA, SAC, and SAB hydrogel beads on the adsorption was shown in Fig. 4. The initial concentration of Cu^{2+} in the solution was 5 mg/L, and the adsorption efficiency of Cu^{2+} in the solution gradually increased with the increase of the dosage of three kinds of hydrogel beads. When the dosage of hydrogel beads reached 4 mg in dry, the adsorption capacity of Cu^{2+} in the solution reached the maximum. Thus, when treating 50 mL wastewater containing Cu^{2+} with a concentration of 5 mg/L, the dosage of hydrogel beads should be used at least 4 mg in dry to achieve adsorption equilibrium, and the adsorption efficiency exceeded 95% under this condition.

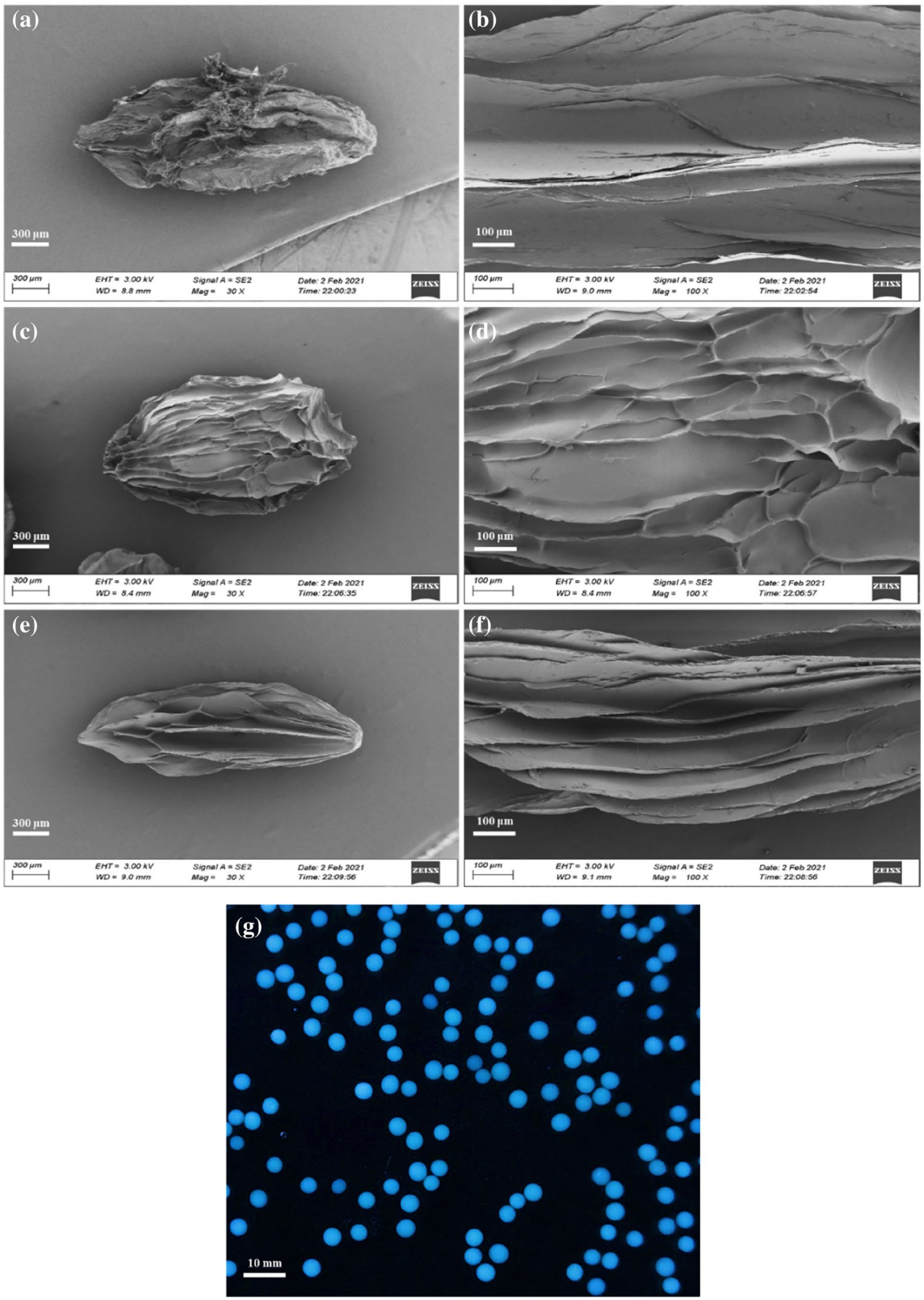

Fig. 1 SEM images of SA (**a**–**b**), SAC (**c**–**d**), SAB (**e**–**f**) and photo (**g**) of sodium alginate hydrogel beads. SA =Cu^{2+} imprinted hydrogel beads prepared with sodium alginate, SAC= Cu^{2+} imprinted hydrogel beads prepared with sodium alginate and carboxymethyl cellulose, SAB= Cu^{2+} imprinted hydrogel beads prepared with sodium alginate and β-cyclodextrin

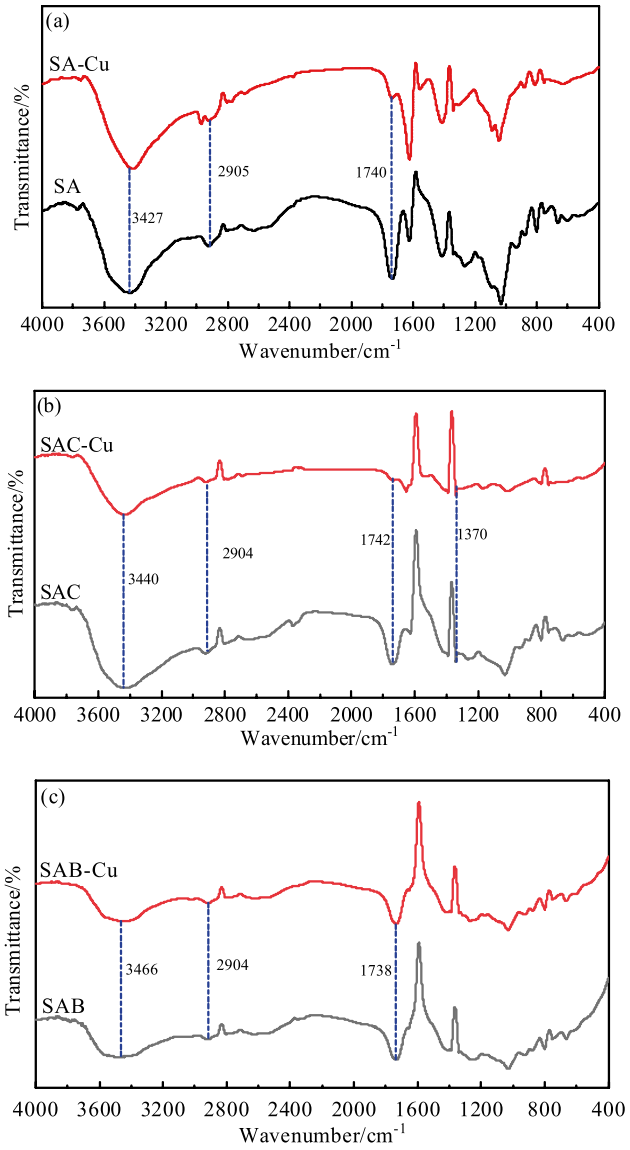

Fig. 2 FT-IR spectra of SA (**a**), SAC (**b**), and SAB (**c**) sodium alginate hydrogel beads before and after adsorption of Cu^{2+}

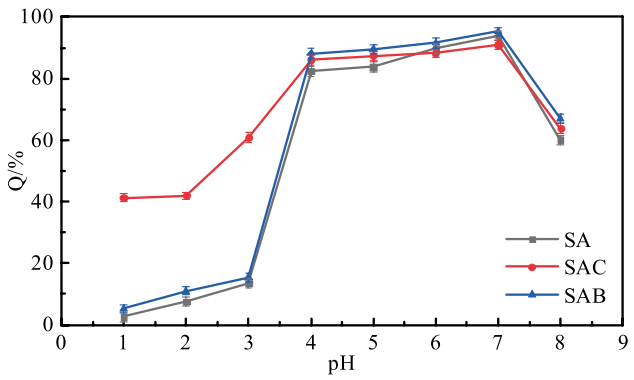

Fig. 3 The effect of pH on the adsorption efficiency of three kinds of hydrogel beads

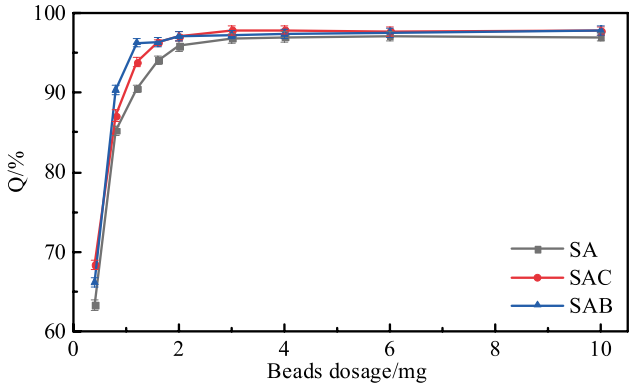

Fig. 4 The effect of the dosage of hydrogel beads on the adsorption

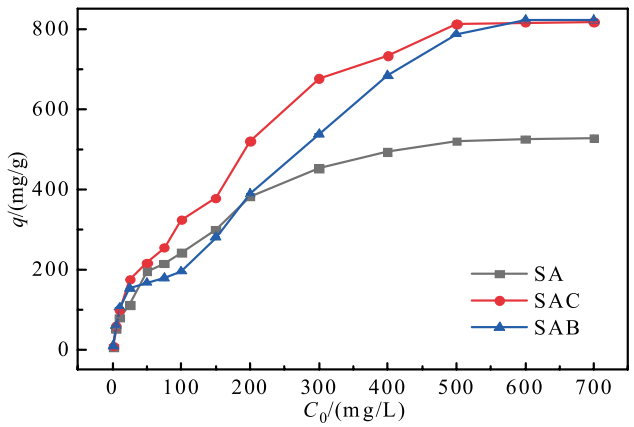

Fig. 5 The effect of initial concentration of Cu^{2+} on adsorption of three hydrogel beads

Effect of Initial Concentration on Adsorption

The adsorption capacity of SA, SAC, and SAB hydrogel beads was also affected by the initial concentration of Cu^{2+} in the solution (Fig. 5). When the concentration of Cu^{2+} was 600 mg/L, the three kinds of hydrogel beads reached the saturated adsorption capacity. The saturated adsorption capacity of sodium alginate hydrogel beads with CMC and β-CD increased significantly with 817 mg/g for SAC beads and 822 mg/g for SAB beads, respectively, which was more than 1.5 times of that of SA beads (510 mg/g). This suggested that the hydrogel beads formed by cross-linking CMC or β-CD with sodium argent alginate play a very important role in metal ion adsorption [29, 31]. More importantly, these values were much higher than the literature reported values for other polymeric hydrogels (Table 1). Thus, the synthesized hydrogel beads with strong adsorption capacity could be a good adsorbent for removing Cu^{2+} from waste water.

Table 1 Saturated adsorption capacities for Cu^{2+} in comparison with previous work

Sample	Saturated adsorption capacity (mg/g)	References
Carboxymethyl cellulose/epichlorohydrin hydrogel	415	[36]
Chitosan entrapped carboxymethylated cellulose hydrogel	45	[46]
Cellulose/gelatin composite hydrogel	52	[47]
Cellulose-graft-polyacrylamide/hydroxyapatite composite hydrogel	175	[48]
Carboxymethyl cellulose/polyacrylamide composite hydrogel	227	[49]
Nanofibrillated cellulose/polyethyleneimine composite hydrogels	175	[50]
Carboxymethyl cellulose-graft-sodium alginate hydrogel imprinted with Cu^{2+}	817	This work
β-cyclodextrin-graft-sodium alginate hydrogel imprinted with Cu^{2+}	822	This work

Adsorption Kinetic Model

Adsorption kinetics controls the rate of adsorption, which determines the time required for reaching equilibrium for the adsorption process. The time to reach equilibrium is also an important data for the development of the process and the adsorption system design [42]. The adsorption kinetics curves of the three kinds of hydrogel beads at 308 K were shown in Fig. 6, the inserted image presented the effect of Cu^{2+} adsorption on the hydrogel beads (Cu^{2+} solution on the left and Cu^{2+} adsorption on the bottom right). The adsorption capacity of Cu^{2+} on the hydrogel beads increased with the increase of adsorption time firstly. The adsorption of SA beads reached equilibrium at about 500 min, SAC beads reached equilibrium at about 250 min, and SAB beads reached equilibrium at about 350 min. It could be concluded that adding CMC and β-CD would shorten the equilibrium time of sodium alginate hydrogel beads.

Kinetic models can give information regarding adsorption pathways and probable mechanism involved [42]. The first-order equation and the second-order equation were used to determine the mass transfer mechanisms and rate-control. Table 2 showed the fitting parameters of quasi-first-order and pseudo-second-order kinetic equations at 308 K. The pseudo-first-order kinetic model for SA beads had higher correlation coefficient than those for SAC and SAB beads, and the calculated q_e of Cu^{2+} on SA beads was very close to that of experimental q_e(exptl.) in three kinds of hydrogel beads, which demonstrated that the adsorption behavior of Cu^{2+} on SA beads could be consistent with the pseudo-first-order kinetic equation, and the adsorption rate of on SA beads was positively correlated to the Cu^{2+} concentration in a certain concentration range.

However, the pseudo-second-order kinetic models for SAC and SAB beads had higher correlation coefficient than that for SA beads, and the calculated q_e of Cu^{2+} on SAC or SAB beads was very close to that of experimental q_e(exptl.), which demonstrated that the adsorption behavior of Cu^{2+} on SAC or SAB beads could be confirmed to the pseudo-second-order kinetic equation, and the adsorption rate of Cu^{2+} on SAC or SAB beads was not only positively correlated with the concentration of adsorbate, but also positively correlated with the amount of adsorbent [43].

Adsorption Isotherm Model

The Langmuir adsorption equation represented the monolayer adsorption process, while Freundlich's adsorption equation introduced the intermolecular force, which represented the multilayer adsorption process [44]. The adsorption isotherm curves of the three kinds of hydrogel beads at 308 K were shown in Fig. 7. And the fitting parameters of Langmuir and Freundlich for adsorption isotherm equations at 308 K were shown in Table 3. The correlation coefficients of the Freundlich adsorption isotherm equation for the three kinds of hydrogel beads are higher than those of Langmuir isotherm equation, and all of q_m, the adsorption amounts of the three kinds of hydrogel beads calculated by the Langmuir adsorption isotherm equation, were tremendously different from the experimental q_e(exptl). The adsorption behavior of Cu^{2+} on gel spherical beads is consistent with the Freundlich adsorption isotherm equation, which indicates that the adsorption of Cu^{2+} by gel spherical beads is a multilayer adsorption process in a certain concentration range.

The Freundlich adsorption isotherm equations of SAC and SAB hydrogel beads had higher correlation coefficients, and it was known that the addition of CMC and β-CD could improve the adsorption capacity of hydrogel beads.

The Adsorptive Selectivity of Cu^{2+} on Hydrogel Beads

For studying the adsorption selectivity of SA, SAC, and SAB hydrogel beads, Cu^{2+} was mixed with 15 coexisting ions (Al^{3+}, Ag^{+}, Ba^{2+}, Ca^{2+}, Cd^{2+}, Co^{2+}, Cr^{3+}, Fe^{2+}, Fe^{3+}, Li^{+}, Mg^{2+}, Mn^{2+}, Ni^{2+}, Pb^{2+} and Zn^{2+}) in the same concentration of 5 mg/L before the adsorption experiment, respectively. The adsorption efficiency of Cu^{2+} [$Q(Cu^{2+})$%] on SA, SAC, and SAB hydrogel beads were the maximum ones, reaching

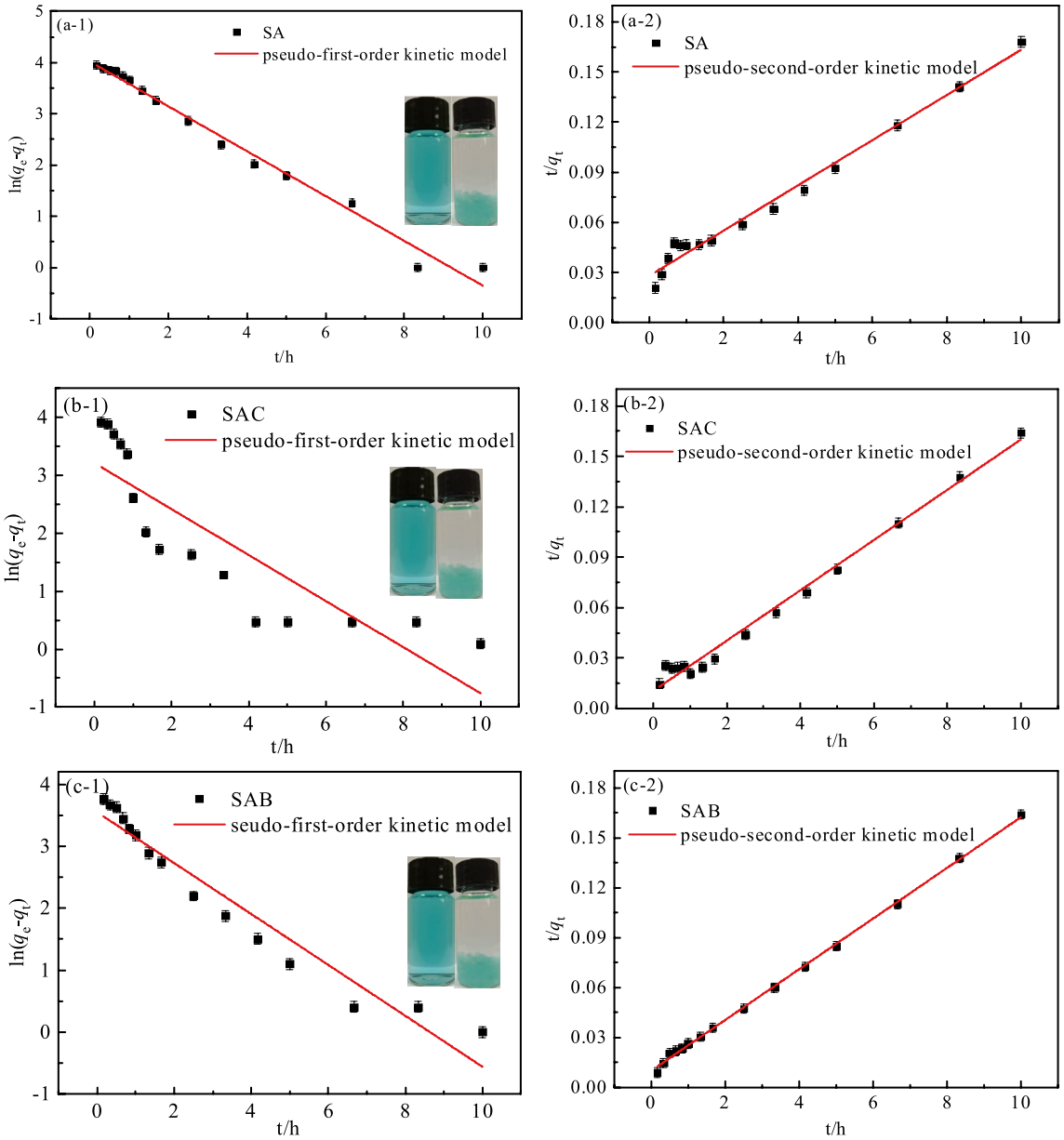

Fig. 6 Adsorption kinetics curve of SA (**a**), SAC (**b**), and SAB (**c**) hydrogel beads

Table 2 Simulation parameters of pseudo-first-order and pseudo-two-order equations for sodium alginate hydrogel beads at 308 K

Materials	q_e(exptl.) (mg/g)	Pseudo-first-order kinetic model			Pseudo-second-order kinetic model		
		q_e(mg/g)	k_1(1/h)	R^2	q_e(mg/g)	k_2[g/(mg/h)]	R^2
SA	59.25 ± 1.56	55.54	0.4372	0.9857	74.07	0.00648	0.9844
SAC	61.56 ± 1.75	24.79	0.3972	0.7536	94.88	0.01063	0.9894
SAB	61.64 ± 2.01	34.35	0.5858	0.9423	65.53	0.02357	0.9989

exptl. experimental

85.1%, 87.0%, and 89.2%, respectively (Fig. 8), while the adsorption efficiency of other coexisting ions on SA, SAC, and SAB hydrogel beads were only from 7.3%–26.9%, 4.8–28.9%, and 1.5–26.1%, respectively (data not shown in Fig. 8). The selectivity of adsorption was identified by the separation factor β [45]. The separation factors of Cu^{2+} to

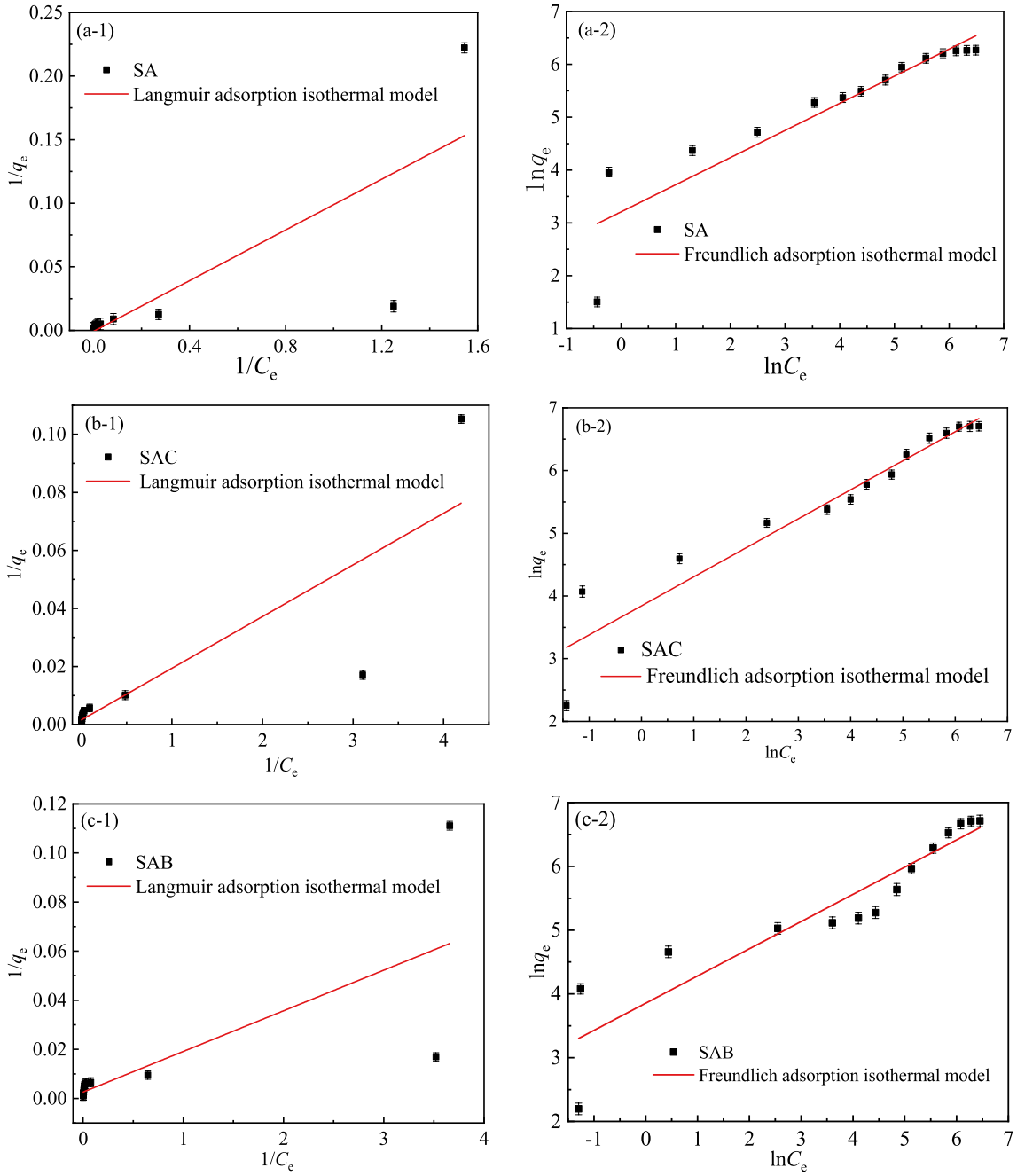

Fig. 7 Adsorption isotherm curve of SA (**a**), SAC (**b**), and SAB (**c**) hydrogel beads

Table 3 Simulation parameters of Langmuir equation and Freundlich equation for adsorption isotherm curve of SA, SAC, and SAB hydrogel beads at 308 K

Materials	q_e(exptl.) (mg/g)	Langmuir adsorption isotherm model			Freundlich adsorption isotherm model		
		q_m (mg/g)	K_L	R_1^2	K_F	m	R_2^2
SA	527.5 ± 5.7	– 1365.65	-7.3519×10^{-3}	0.6856	8.7216	0.5134	0.8453
SAC	817.3 ± 6.4	625.00	8.9888×10^{-2}	0.5743	10.4431	0.4629	0.8642
SAB	822.6 ± 6.3	384.62	0.1566	0.7510	10.4792	0.4265	0.9210

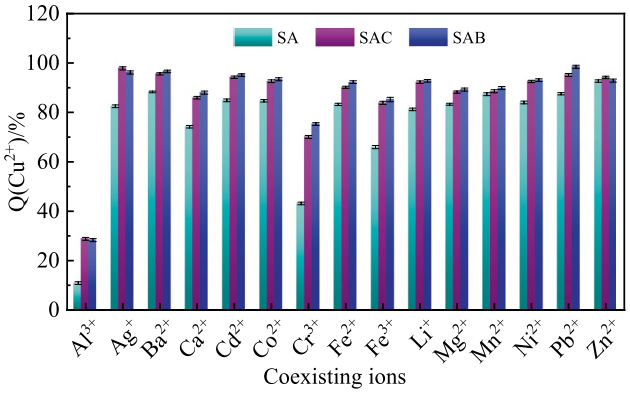

Fig. 8 The adsorptive selectivity of Cu^{2+} on SA, SAC, and SAB hydrogel beads

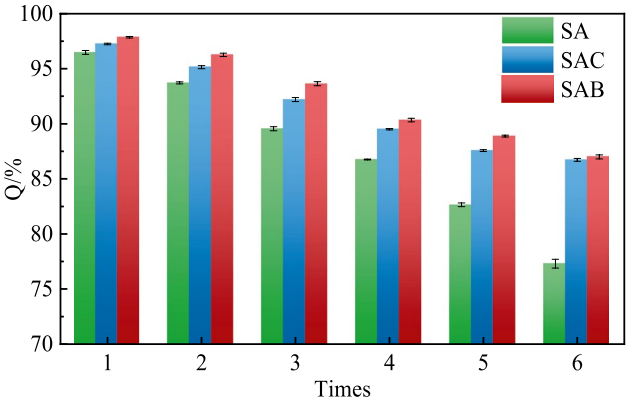

Fig. 9 The recycling times of SA, SAC, and SAB hydrogel beads adsorption/desorption to Cu^{2+}

other ions $\beta(Cu^{2+}$/other ions) was 3.2–11.7 for SA beads, $\beta(Cu^{2+}$/other ions) was 3.0–18.1 for SAC, and $\beta(Cu^{2+}$/other ions) was 3.4–59.5 for SAB, which reflected the adsorption separation abilities of SA, SAC, and SAB hydrogel beads between Cu^{2+} and other coexisting ions. Thus, the SA, SAC, and SAB hydrogel beads prepared with Cu^{2+} as template, especially SAB beads, show better selectivity for Cu^{2+} than other coexisting ions.

Cycling and Regeneration

Figure 9 showed the effect of HCl solution on the desorption and regeneration of Cu^{2+} adsorbed sodium alginate hydrogel beads. Although the adsorbent maintained its original morphology with the increase of elution time, the desorption-adsorption process caused some damage inside the adsorbent, resulting in a gradual decrease in the adsorption efficiency of Cu^{2+} on the hydrogel beads, the adsorption efficiency of Cu^{2+} on the SAC and SAB hydrogel beads remained above 88% after recycling desorption-adsorption process for six times, while the adsorption efficiency of SA hydrogel beads decreased to below 80%. All above-mentioned results proved that the hydrogel beads synthesized by our proposed method possessed high specific adsorption, selectivity, and reusability.

Conclusions

In this study, to realize the specific adsorption and removal of Cu^{2+} from wastewater, three kinds of environmentally friendly Cu^{2+} ion-imprinted hydrogel beads with high adsorption capacity and high selectivity for Cu^{2+} were successfully prepared using natural raw materials such as sodium alginate. In the process of preparing ion-imprinted sodium alginate hydrogel beads, blending with carboxymethyl cellulose or β-cyclodextrin could improve the saturated adsorption capacity of Cu^{2+}. Thus, ion-imprinted sodium alginate hydrogel beads, especially enhanced with carboxymethyl cellulose or β-cyclodextrin can be developed and utilized as a new type of adsorption material for heavy metal. Once the adsorption achieves saturation, the copper could be recycled by electrochemical treatment or burning treatment of the absorbed beads, which should be investigated further.

Acknowledgements The authors acknowledge the financial support of the Provincial Key Research and Development Plan in Hunan, China (2020NK2019), the National Natural Science Foundation for Young Scientists of China (22004132), and the Natural Science Foundation of Hunan Province, China (2020JJ4940). All authors appreciate the editors and the anonymous reviewers for their constructive comments and critical evaluation.

Author Contributions All authors contributed to the study conception and design. YF: data curation, investigation, methodology, writing original draft. DS: investigation, project administration, writing original draft. YY: methodology, writing review and editing. XH: project administration, writing original draft. YG: formal analysis, funding acquisition. YZ: formal analysis, writing original draft. ZL: writing review and editing. LX: funding acquisition, supervision, writing review and editing. All authors read and approved the final manuscript.

Declarations

Conflict of interest The authors declared that they have no conflicts of interest to this work.

References

1. Ashraf S, Cluley A, Mercado C, Mueller A (2011) Imprinted polymers for the removal of heavy metal ions from water. Water Sci Technol 64(6):1325–1332. https://doi.org/10.2166/wst.2011.423
2. Joseph L, Jun B-M, Flora JRV, Park CM, Yoon Y (2019) Removal of heavy metals from water sources in the developing world using low-cost materials: a review. Chemosphere 229:142–159. https://doi.org/10.1016/j.chemosphere.2019.04.198

3. Wolowiec M, Komorowska-Kaufman M, Pruss A, Rzepa G, Bajda T (2019) Removal of heavy metals and metalloids from water using drinking water treatment residuals as adsorbents: a review. Minerals 9(8):487. https://doi.org/10.3390/min9080487
4. Hashim MA, Mukhopadhyay S, Sahu JN, Sengupta B (2011) Remediation technologies for heavy metal contaminated groundwater. J Environ Manag 92(10):2355–2388. https://doi.org/10.1016/j.jenvman.2011.06.009
5. Mao G, Zhao Y, Zhang F, Liu J, Huang X (2019) Spatiotemporal variability of heavy metals and identification of potential source tracers in the surface water of the Lhasa River basin. Environ Sci Pollut Res 26(8):7442–7452. https://doi.org/10.1007/s11356-019-04188-0
6. Yu M, Zhang J, Tian Y (2018) Change of heavy metal speciation, mobility, bioavailability, and ecological risk during potassium ferrate treatment of waste-activated sludge. Environ Sci Pollut Res 25(14):13569–13578. https://doi.org/10.1007/s11356-018-1511-7
7. Bashir A, Malik LA, Ahad S, Manzoor T, Bhat MA, Dar GN, Pandith AH (2019) Removal of heavy metal ions from aqueous system by ion-exchange and biosorption methods. Environ Chem Lett 17(2):729–754. https://doi.org/10.1007/s10311-018-00828-y
8. Liu Y, Zhang Z (2018) Preparation of polymeric adsorbent and study of Its adsorption of heavy metal ions in water. J Coast Res 83:414–417. https://doi.org/10.2112/si83-069.1
9. Butter B, Santander P, Pizarro GdC, Oyarzun DP, Tasca F, Sanchez J (2021) Electrochemical reduction of Cr(VI) in the presence of sodium alginate and its application in water purification. J Environ Sci 101:304–312. https://doi.org/10.1016/j.jes.2020.08.033
10. Jugnia L-B, Manno D, Hendry M, Tartakovsky B (2019) Removal of heavy metals in a flow-through vertical microbial electrolysis cell. Can J Chem Eng 97(10):2608–2616. https://doi.org/10.1002/cjce.23568
11. Alam MM, Alothman ZA, Naushad M, Aouak T (2014) Evaluation of heavy metal kinetics through pyridine based Th(IV) phosphate composite cation exchanger using particle diffusion controlled ion exchange phenomenon. J Ind Eng Chem 20(2):705–709. https://doi.org/10.1016/j.jiec.2013.05.036
12. El-Sheikh SM, Azzam AB, Geioushy RA, El Dars FM, Salah BA (2021) Visible-light-driven 3D hierarchical Bi_2S_3/BiOBr hybrid structure for superior photocatalytic Cr(VI) reduction. J Alloys Compd 857:157513. https://doi.org/10.1016/j.jallcom.2020.157513
13. Geioushy RA, El-Sheikh SM, Azzam AB, Salah BA, El-Dars FM (2020) One-pot fabrication of $BiPO_4$/Bi_2S_3 hybrid structures for visible-light driven reduction of hazardous Cr(VI). J Hazard Mater 381:120955. https://doi.org/10.1016/j.jhazmat.2019.120955
14. Rafique M, Hajra S, Tahir MB, Gillani SSA, Irshad M (2022) A review on sources of heavy metals, their toxicity and removal technique using physico-chemical processes from wastewater. Environ Sci Pollut Res 29(11):16772–16781. https://doi.org/10.1007/s11356-022-18638-9
15. Parveen N, Zaidi S, Danish M (2017) Development of SVR-based model and comparative analysis with MLR and ANN models for predicting the sorption capacity of Cr(VI). Process Saf Environ Prot 107:428–437. https://doi.org/10.1016/j.psep.2017.03.007
16. Kaur K, Jindal R, Tanwar R (2019) Chitosan-gelatin @ Tin (IV) tungstatophosphate nanocomposite ion exchanger: synthesis, characterization and applications in environmental remediation. J Polym Environ 27(1):19–36. https://doi.org/10.1007/s10924-018-1321-5
17. Wu Y, Chen J, Che H, Gao X, Ao Y, Wang P (2022) Boosting 2e(-) oxygen reduction reaction in garland carbon nitride with carbon defects for high-efficient photocatalysis-self-Fenton degradation of 2,4-dichlorophenol. Appl Catal B. https://doi.org/10.1016/j.apcatb.2022.121185
18. Abu Al-Rub FA, Fares MM, Talafha T (2018) Poly(acrylic acid) grafted sodium alginate di-block hydrogels as efficient biosorbents; structure-property relevance. J Polym Environ 26(6):2333–2345. https://doi.org/10.1007/s10924-017-1104-4
19. Gao X, Guo C, Hao J, Zhao Z, Long H, Li M (2020) Adsorption of heavy metal ions by sodium alginate based adsorbent-a review and new perspectives. Int J Biol Macromol 164:4423–4434. https://doi.org/10.1016/j.ijbiomac.2020.09.046
20. Rajput A, Sharma PP, Yadav V, Gupta H, Kulshrestha V (2019) Synthesis and characterization of different metal oxide and GO composites for removal of toxic metal ions. Sep Sci Technol 54(3):426–433. https://doi.org/10.1080/01496395.2018.1500596
21. Ablouh E-h, Hanani Z, Eladlani N, Rhazi M, Taourirte M (2019) Chitosan microspheres/sodium alginate hybrid beads: an efficient green adsorbent for heavy metals removal from aqueous solutions. Sustain Environ Res. https://doi.org/10.1186/s42834-019-0004-9
22. Kolodynska D, Geca M, Skwarek E, Goncharuk O (2018) Titania-coated silica alone and modified by sodium alginate as sorbents for heavy metal ions. Nanoscale Res Lett. https://doi.org/10.1186/s11671-018-2512-7
23. Velempini T, Pillay K, Mbianda XY, Arotiba OA (2017) Epichlorohydrin crosslinked carboxymethyl cellulose-ethylenediamine imprinted polymer for the selective uptake of Cr(VI). Int J Biol Macromol 101:837–844. https://doi.org/10.1016/j.ijbiomac.2017.03.048
24. Fu J, Wang X, Li J, Chen L (2016) Ion imprinting technology for heavy metal ions. Progress Chem 28(1):83–90. https://doi.org/10.7536/pc150742
25. Jing H, Huang X, Du X, Mo L, Ma C, Wang H (2022) Facile synthesis of pH-responsive sodium alginate/carboxymethyl chitosan hydrogel beads promoted by hydrogen bond. Carbohydr Polym. https://doi.org/10.1016/j.carbpol.2021.118993
26. Feng Y, Wang Y, Wang Y, Zhang X-F, Yao J (2018) In-situ gelation of sodium alginate supported on melamine sponge for efficient removal of copper ions. J Colloid Interface Sci 512:7–13. https://doi.org/10.1016/j.jcis.2017.10.036
27. Ren H, Gao Z, Wu D, Jiang J, Sun Y, Luo C (2016) Efficient Pb(II) removal using sodium alginate-carboxymethyl cellulose gel beads: Preparation, characterization, and adsorption mechanism. Carbohydr Polym 137:402–409. https://doi.org/10.1016/j.carbpol.2015.11.002
28. Dong W, Pu X, Zhai Y, Yin Q (2020) The treatment of high-heavy metal ion-containing waste drilling fluid by β-cyclodextrin/bentonite. Ind Water Treatm 40(3):27–30. https://doi.org/10.11894/iwt.2019-0274
29. Ali ASM, El-Aassar MR, Hashem FS, Moussa NA (2019) Surface modified of cellulose acetate electrospun nanofibers by polyaniline/beta-cyclodextrin composite for removal of cationic dye from aqueous medium. Fibers Polym 20(10):2057–2069. https://doi.org/10.1007/s12221-019-9162-y
30. Guan M, Bi H, Wang Z, Bu S, Huang L, Yang LI (2013) Synthesis, characterization and the applicability of β-cyclodextrins functionalized mesoporous SBA-15 molecular sieves. NANO 8(5):34–40. https://doi.org/10.1142/S1793292013500501
31. Musarurwa H, Tavengwa NT (2020) Application of carboxymethyl polysaccharides as bio-sorbents for the sequestration of heavy metals in aquatic environments. Carbohydr Polym 237:116142. https://doi.org/10.1016/j.carbpol.2020.116142
32. Ding Q, Chen H, Huang C, Lu Q, Tong P, Zhang W, Zhang L (2020) A fish scale-like magnetic nanomaterial as a highly efficient sorbent for monitoring the changes in auxin levels under cadmium stress. Analyst 145(17):5925–5932. https://doi.org/10.1039/d0an00269k
33. Lan W, He L, Liu Y (2018) Preparation and properties of sodium carboxymethyl cellulose/sodium alginate/chitosan composite film. Coatings 8(8):291. https://doi.org/10.3390/coatings8080291

34. Hu X, Hu Y, Xu G, Li M, Zhu Y, Jiang L, Tu Y, Zhu X, Xie X, Li A (2020) Green synthesis of a magnetic β-cyclodextrin polymer for rapid removal of organic micro-pollutants and heavy metals from dyeing wastewater. Environ Res 180:108796. https://doi.org/10.1016/j.envres.2019.108796
35. Tang S, Yang J, Lin L, Peng K, Chen Y, Jin S, Yao W (2020) Construction of physically crosslinked chitosan/sodium alginate/calcium ion double-network hydrogel and its application to heavy metal ions removal. Chem Eng J 393:124728. https://doi.org/10.1016/j.cej.2020.124728
36. Yang S, Fu S, Liu H, Zhou Y, Li X (2011) Hydrogel beads based on carboxymethyl cellulose for removal heavy metal ions. J Appl Polym Sci 119(2):1204–1210. https://doi.org/10.1002/app.32822
37. Tao H, Li S, Zhang L, Chen Y, Deng L (2019) Magnetic chitosan/sodium alginate gel bead as a novel composite adsorbent for Cu(II) removal from aqueous solution. Environ Geochem Health 41(1):297–308. https://doi.org/10.1007/s10653-018-0137-5
38. He J, Dai J, Xie A, Tian S, Chang Z, Yan Y, Huo P (2016) Preparation of macroscopic spherical porous carbons@carboxymethylcellulose sodium gel beads and application for removal of tetracycline. RSC Adv 6(87):84536–84546. https://doi.org/10.1039/c6ra14877h
39. Zhang H, Omer AM, Hu Z, Yang L-Y, Ji C, Ouyang X-K (2019) Fabrication of magnetic bentonite/carboxymethyl chitosan/sodium alginate hydrogel beads for Cu(II) adsorption. Int J Biol Macromol 135:490–500. https://doi.org/10.1016/j.ijbiomac.2019.05.185
40. Al-Musawi TJ, Mengelizadeh N, Al Rawi O, Balarak D (2022) Capacity and modeling of acid blue 113 dye adsorption onto chitosan magnetized by Fe_2O_3 nanoparticles. J Polym Environ 30(1):344–359. https://doi.org/10.1007/s10924-021-02200-8
41. Sarmast ZMS, Sedaghat S, Derakhshi P, Azar PA (2022) Facile fabrication of silver nanoparticles grafted with Fe_3O_4-chitosan for efficient removal of amoxicillin from aqueous solution: application of central composite design. J Polym Environ 30(7):2990–3004. https://doi.org/10.1007/s10924-022-02402-8
42. Freyria FS, Sannino F, Bonelli B (2020) Chapter 2 - Common wastewater contaminants versus emerging ones: an overview. In: Bonelli B, Freyria FS, Rossetti I, Sethi R (eds) Nanomaterials for the detection and removal of wastewater pollutants. Elsevier, Amsterdam, pp 19–46
43. Wang B, Deng H, Wu M, Xiang S, Ma Q, Shi S, Xie L, Guo Y (2018) Magnetic surface molecularly imprinted polymeric microspheres using gallic acid as a segment template for excellent recognition of ester catechins. Anal Methods 10(27):3317–3324. https://doi.org/10.1039/c8ay00903a
44. Wu M, Fan Y, Li J, Lu D, Guo Y, Xie L, Wu Y (2019) Vinyl phosphate-functionalized, magnetic, molecularly-imprinted polymeric microspheres' enrichment and carbon dots' fluorescence-detection of organophosphorus pesticide residues. Polymers 11:11. https://doi.org/10.3390/polym11111770
45. Deng H, Wang B, Wu M, Deng B, Xie L, Guo Y (2019) Rapidly colorimetric detection of caffeine in beverages by silver nanoparticle sensors coupled with magnetic molecularly imprinted polymeric microspheres. Int J Food Sci Technol 54(1):202–211. https://doi.org/10.1111/ijfs.13924
46. Zhao L, Mitomo H (2008) Adsorption of heavy metal ions from aqueous solution onto chitosan entrapped CM-cellulose hydrogels synthesized by irradiation. J Appl Polym Sci 110(3):1388–1395. https://doi.org/10.1002/app.28718
47. Teow YH, Kam LM, Mohammad AW (2018) Synthesis of cellulose hydrogel for copper (II) ions adsorption. J Environ Chem Eng 6(4):4588–4597. https://doi.org/10.1016/j.jece.2018.07.010
48. Saber-Samandari S, Saber-Samandari S, Gazi M (2013) Cellulose-graft-polyacrylamide/hydroxyapatite composite hydrogel with possible application in removal of Cu(II) ions. React Funct Polym 73:1523–1530. https://doi.org/10.1016/j.reactfunctpolym.2013.07.007
49. Godiya CB, Cheng X, Li D, Chen Z, Lu X (2019) Carboxymethyl cellulose/polyacrylamide composite hydrogel for cascaded treatment/reuse of heavy metal ions in wastewater. J Hazard Mater 364:28–38. https://doi.org/10.1016/j.jhazmat.2018.09.076
50. Li J, Zuo K, Wu W, Xu Z, Yi Y, Jing Y, Dai H, Fang G (2018) Shape memory aerogels from nanocellulose and polyethyleneimine as a novel adsorbent for removal of Cu(II) and Pb(II). Carbohydr Polym 196:376–384. https://doi.org/10.1016/j.carbpol.2018.05.015